

**Zeitschrift:** IABSE reports = Rapports AIPC = IVBH Berichte  
**Band:** 999 (1997)  
  
**Artikel:** Prediction of cumulative damage in SRC beam-columns  
**Autor:** Uchida, Yasuhiro / Kojo, Yasuhiko / Bochi, Akito  
**DOI:** <https://doi.org/10.5169/seals-1038>

### **Nutzungsbedingungen**

Die ETH-Bibliothek ist die Anbieterin der digitalisierten Zeitschriften auf E-Periodica. Sie besitzt keine Urheberrechte an den Zeitschriften und ist nicht verantwortlich für deren Inhalte. Die Rechte liegen in der Regel bei den Herausgebern beziehungsweise den externen Rechteinhabern. Das Veröffentlichen von Bildern in Print- und Online-Publikationen sowie auf Social Media-Kanälen oder Webseiten ist nur mit vorheriger Genehmigung der Rechteinhaber erlaubt. [Mehr erfahren](#)

### **Conditions d'utilisation**

L'ETH Library est le fournisseur des revues numérisées. Elle ne détient aucun droit d'auteur sur les revues et n'est pas responsable de leur contenu. En règle générale, les droits sont détenus par les éditeurs ou les détenteurs de droits externes. La reproduction d'images dans des publications imprimées ou en ligne ainsi que sur des canaux de médias sociaux ou des sites web n'est autorisée qu'avec l'accord préalable des détenteurs des droits. [En savoir plus](#)

### **Terms of use**

The ETH Library is the provider of the digitised journals. It does not own any copyrights to the journals and is not responsible for their content. The rights usually lie with the publishers or the external rights holders. Publishing images in print and online publications, as well as on social media channels or websites, is only permitted with the prior consent of the rights holders. [Find out more](#)

**Download PDF:** 14.12.2025

**ETH-Bibliothek Zürich, E-Periodica, <https://www.e-periodica.ch>**

## Prediction of Cumulative Damage in SRC Beam-Columns

**Yasuhiro UCHIDA**  
Associate Professor  
Kagoshima University  
Kagoshima, Japan

**Yasuhiko KOJO**  
Civil Engineer  
Nishimatsu construction  
Tokyo, Japan

**Akito BOCHI**  
Research Student  
Kagoshima University  
Kagoshima, Japan

### Summary

The critical axial force for convergence-axial displacement curves of SRC and RC beam-columns are proposed as a characteristic curves for repeated loading in order to predict the cumulative damage. Tests and analyses of SRC and RC beam-columns were carried out and it was found that the cumulative damage could be evaluated by the curves very well.

### 1. Introduction

Since the strong horizontal force occurred in earthquake often causes the cumulative damage such as the strength deterioration and the accumulation of deformation in structures and their members, the prediction of cumulative damage is needed in the aseismic design of structures. In this study, the characteristic curves of composite steel and reinforced concrete (SRC) beam-columns are presented experimentally and analytically, and a method of predicting convergence-divergence phenomena in accumulation of deformation of beam-columns is explained.

### 2. Evaluation of Cumulative Damage by Characteristic Curve for Cyclic Loading

The strength deterioration and the accumulation of deformation in structures subjected to repeated loading are named cumulative damage in this study. Since the deteriorating behavior closely correlates with the accumulation of deformation, it is necessary to investigate the accumulation of deformation. A limit value of the axial force when the accumulation of deformation in a beam-column subjected to a repeated horizontal force converges to a certain value is named critical axial force for convergence. Since "critical axial force for convergence" is very long, it is termed "critical axial force" hereafter.

Procedures of obtaining the critical axial force of a beam-column are outlined as follows;

- 1) Give a value of converged axial displacement.
- 2) Apply an axial force so that the value of axial displacement may become a given value.
- 3) Apply a repeated horizontal force with a given constant displacement amplitude under the given axial displacement.
- 4) The minimum axial force obtained in the loading step 3) gives a critical axial force.
- 5) Increase the value of converged axial displacement and go to 1).

In general, the critical axial force is approximately given by the minimum value of axial force under an assumed axial displacement, because the varying axial force become a true one when it takes an extreme value, which can be derived from theorem of minimum potential energy. The relation between the critical axial force and the maximum of displacement varying in the converged state becomes the critical axial force-axial displacement relation.

### 3. Critical Axial Forces of RC and SRC Beam-Columns

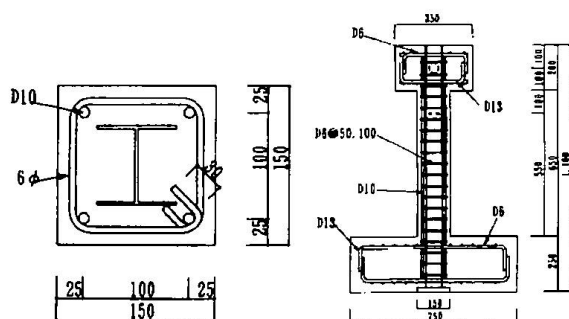
#### 3.1 Experiments

##### 3.1.1 Specimens and Mechanical Properties

RC and SRC specimens were tested under a axial force and a repeated horizontal force. Figure 2 exhibits the configuration and dimensions of SRC specimens, and those are same as ones of RC specimens except for the encased steel. Depth and width of SRC cross section are 150mm. In SRC specimens, an H-section of steel H-75x75x3.2x3.2 (mm) built up by welding is encased in concrete with 4 deformed main bars. Hoops of D6 are placed with a pitch of 50mm in bending failure type RC specimens and SRC specimens and with a pitch of 100mm in shear failure type RC specimens. Table 1 shows measured dimensions, compression strength of concrete, hoop ratio and spacing of hoops. The material properties of reinforced bars and steel are listed in Table 2. Specimens RC1~RC3 and SRC1~SRC2 are bending failure type specimens with hoop ratio  $\rho_p=0.85\%$  and Specimens RC4~RC6 shear failure type ones with  $\rho_p=0.43\%$ .

##### 3.1.2 Experimental Method

RC and SRC beam-columns under a repeated horizontal force and an axial force were tested. Figure 2 shows a test set-up. Specimens were fixed at its end horizontally to the loading frame because the height of the loading frame is not sufficient for erecting the apparatus vertically.



(a) Cross Section (b) Elevation  
Fig. 1 SRC specimen

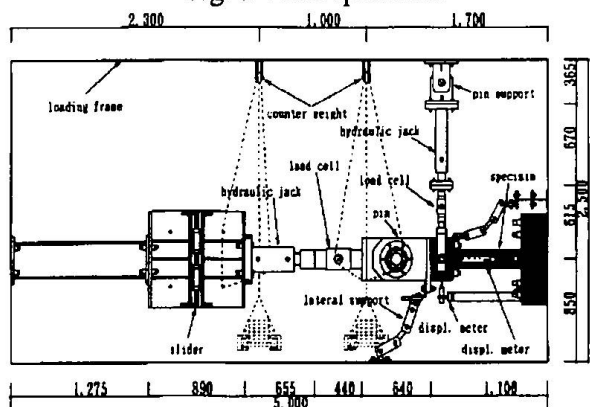


Fig. 2 Test set-up

Table 1 Experimental Parameters

Spec. No.	B (mm)	D (mm)	$\ell$ (mm)	h (mm)	$F_c$ (kg/cm <sup>2</sup> )	$\rho_p$ (%)	x (mm)
RC1	149.2	151.2	750.1	549.4	412	0.85	50
RC2	149.0	153.1	751.7	550.0	339	0.85	50
RC3	150.1	152.1	751.0	548.7	407	0.85	50
RC4	150.6	150.5	749.7	549.9	446	0.43	100
RC5	150.3	150.6	750.6	549.3	401	0.43	100
RC6	151.7	151.6	749.2	549.1	420	0.43	100
SRC1	148.5	150.5	750.0	550.5	388	0.85	50
SRC2	149.0	149.8	748.3	552.5	378	0.85	50

B=width, D=depth of cross section  
 $\ell$ =length,  $F_c$ =compression strength  
 $\rho_p$ =hoop ratio, x=spacing of hoops

Table 2 Material properties

Materials		$\sigma_y$ (t/cm <sup>2</sup> )	$\sigma_u$ (t/cm <sup>2</sup> )	$\delta$ (%)
Re-Bars	D-6	3.96	6.11	18.4
	D-10	3.56	5.22	20.2
	D-13	3.44	5.02	19.4
Steel H-75x75x3.2x3.2		3.73	4.6	20.6

$\sigma_y$ =yield stress,  $\sigma_u$ =tensile strength  
 $\delta$ =elongation

Repeated horizontal force with a constant displacement amplitude of 10mm was applied to the top of the beam-column by a hydraulic jack and an axial force was also applied to that through a pin. Here the horizontal force means the force in the direction perpendicular to the axial direction of the specimen. The hydraulic jack for axial loading was attached to a slider so that the axial compressive and tensile force can be applied with moving.

Critical axial forces were obtained by two kinds of loading. To Specimens RC2 and RC5, a repeated horizontal force was applied in three cycles successively with keeping the axial displacement constant (Test 1). The critical axial force can be given by the minimum value of the axial force in the third cycle. In Specimens RC3 and RC4, critical axial forces were obtained by providing the variable axial displacement assumed on the base of displacement in the previous step (Test 2). The convergence-divergence behavior of axial deformation was investigated under an axial force varied in the stepwise manner in the vicinity of the critical axial force-displacement relation in order to verify the validity of the critical axial force obtained by Test 1 and Test 2. The horizontal displacement  $\delta_h$  at the top of specimens was measured by a displacement meter installed on the stand and the axial displacement  $\delta_v$  by displacement meters equipped on sliders set up between both ends of the specimen. The measured displacement  $\delta_v$  is, however, not a vertical displacement but a displacement in the axial direction of the specimen.

### 3.13 Test Results and Discussions

Figs. 3 through 9 exhibit test results of RC and SRC specimens. The axial force  $p$ -axial displacement  $\delta_v$  relations of Specimens RC2 and RC5 is shown in Fig. 3 where open squares represents the maximum point of varying axial force-minimum axial displacement, and open circles the minimum point of varying axial force-maximum axial displacement. Figure 3(a) is a result for bending failure type specimens and Fig. 3(b) for shear failure type specimens.  $p$  in these figures is the axial force normalized by  $F_c BD$  in which  $F_c$  denotes compressive strength, and  $B$  and  $D$  denote width and depth of the cross section. Open circles and solid circles in Figs. 4(a) and (b) indicate the axial force  $p$ -axial displacement  $\delta_v$  relations of bending failure type Specimen RC1 and shear failure type Specimen RC6 subjected to a constant axial force in a stepwise manner. The solid line in these figures indicate the critical axial force-axial displacement relation expressed by the inner curve formed by curves with open squares and open circles. The stages of constant axial force loading are designated by 1~10 and 1~8. Open circles and solid circles in the loading stage represents convergence and divergence in the accumulation of deformation, respectively. Figs. 5 and 6 show the critical axial force-axial displacement relation and the accumulation of deformation under a constant axial force for Specimens SRC1 and SRC2. The axial force of SRC specimens is normalized by the axial ultimate strength  $\{c_y F_c BD + A_s \sigma_y + a_s \sigma_y\}$  where  $\sigma_y$ =yield stress of reinforced bar,  $c_y = 0.85-2.5 p_c$ ,  $p_c = a_s / BD$ ,  $a_s$ =area of a steel flange,  $\sigma_y$ =yield stress of steel,  $A_s$ =area of the encased steel,  $a_s$ =total area of reinforced bar.

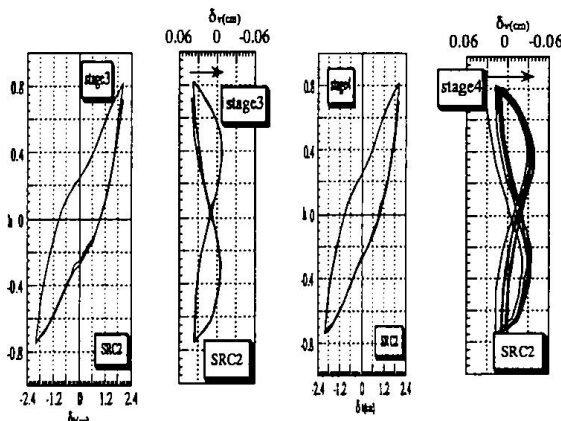
Figures 7(a) and (b) are horizontal force  $h$ -horizontal displacement  $\delta_h$  relations for bending failure type Specimens RC1 under constant axial forces  $p = -0.18$  (loading stage 3 in Fig. 4 (a)) and  $-0.26$  (stage 4), and Figs. 8(a) and (b) for shear failure type Specimens RC6 under constant axial forces  $p = -0.33$  (stage 4 in Fig. 4(b)) and  $p = -0.41$  (stage 5). Hysteresis loops of Specimen SRC2 under  $p = -0.17$  (stage 3 in Fig. 6) and  $p = -0.23$  (stage 4) are shown in Fig. 9(a) and (b), respectively. Horizontal force  $h$  of RC and SRC specimens are normalized by ultimate strengths  $\{a_s \sigma_y (D-2d_c) + 0.12 BD^2 F_c\} / \ell$  and  $\{c_y BD^2 F_c / 8 + Z_p \sigma_y + a_s \sigma_y (D-2d_c)\}$  prescribed in A.I.J standards, respectively, where  $a_s$ =total area of tension reinforced bars,  $d_c$ =depth of cover concrete,  $\ell$ =length of specimen,  $Z_p$ =plastic section modulus of steel.

The accumulation of deformation converges and the hysteresis loop closes in the beam-column under a axial force less than the maximum critical axial force (Figs. 3 through 9). In the beam-column under a axial force greater the maximum critical axial force, however, the cumulative damage increases with the divergent accumulation of deformation and strength deterioration due to bending failure or shear failure. Figures 3 through 9 show that the critical axial force  $p$ -axial displacement  $\delta_v$  relation forms a hysteresis and the strength deterioration and the accumulation of deformation increase with the increase in the slope of the descending  $p$ - $\delta_v$  curve. Therefore, it is noted that the progress of strength deterioration and the convergence-divergence behavior in

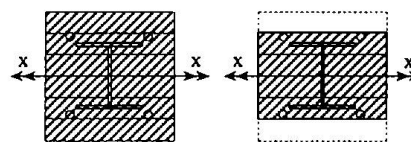
the accumulation of deformation are predictable by  $p_{cr}-\delta_v$  curves.

### 3.2 Analyses

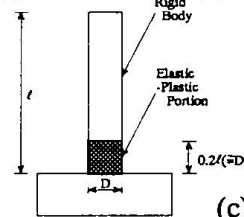
Analytical models of SRC beam-columns are shown in Fig. 10. Models of RC beam-columns are identical with that of SRC beam-columns except for the encased steel. Cross sections of models are divided into a number of segments and are idealized in Model A (Fig. 10(a)) of the gross cross section and Model B (Fig. 10(b)) of cross section without cover concretes in consideration of spalling due to compression. Fig. 10(c) exhibits the analytical model of beam-columns which consists of an elastic-plastic portion and a rigid body. The length of the elastic-plastic portion is  $0.2\ell$  and is the depth of cross section  $D$  approximately, where  $\ell$  is the length of beam-column. Figures 11(a) and (b) show an assumed stress-strain relation of the reinforced bar, steel and concrete, in which the tension is taken positive. Stress 's' of concrete is normalized by compression strength and stresses of reinforced bar and steel are normalized by yield ones. Strains are also normalized in the same way as stresses. Skeleton curve of stress-strain relations of concrete are expressed as a function  $f_1(e)$  as shown in Eq. (1). The strain  $e_u$  at the ultimate point of the stress-strain relation was assumed to be -3.



(a)  $p=-0.17$ , conv. (b)  $p=-0.23$ , div.  
Fig. 9 Hysteresis loops of SRC beam-columns

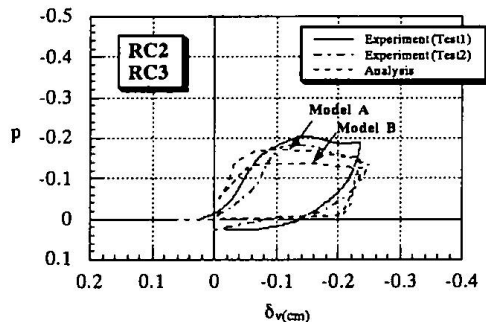


(a) Model A (b) Model B

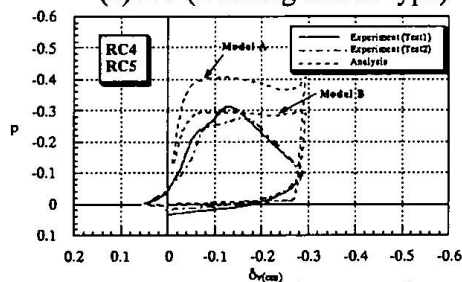


(c) Beam-column

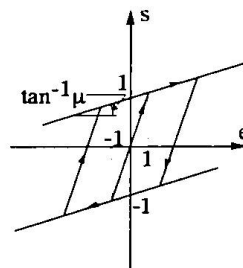
Fig. 10 Analytical models



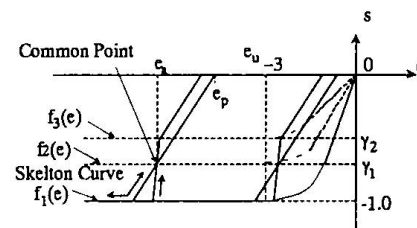
(a) RC (Bending failure type)



(b) RC (Shear failure type)

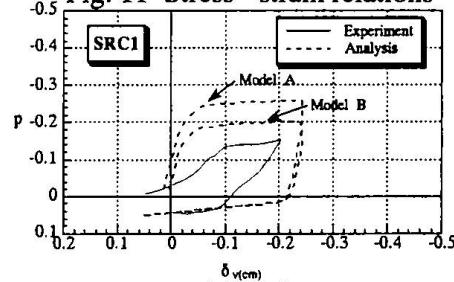


(a) Re-bars and steel



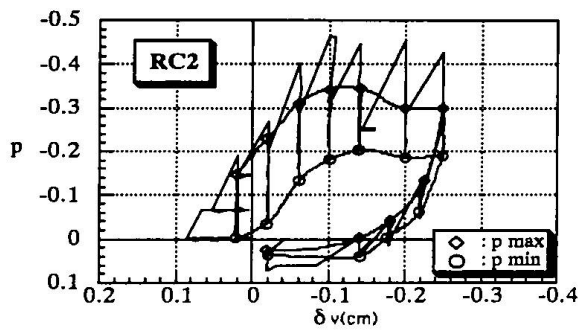
(b) Concrete

Fig. 11 Stress - strain relations

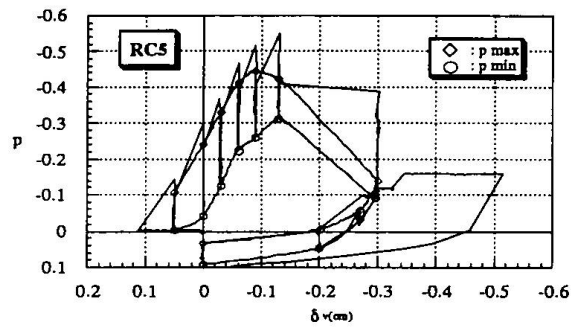


(c) SRC

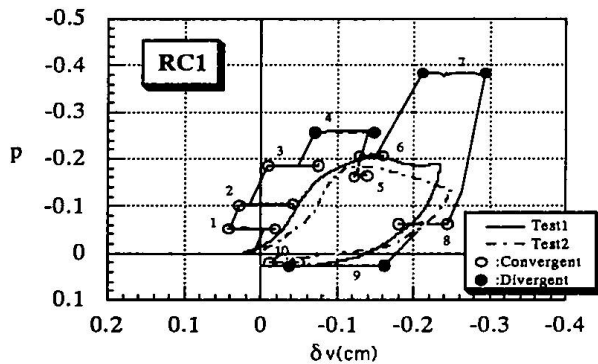
Fig. 12 Comparison between  $p_{cr}-\delta_v$  curves obtained by tests and analyses



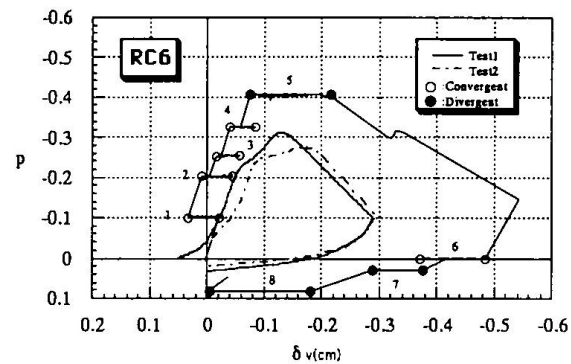
(a) Bending failure



(b) Shear failure

Fig. 3  $p_{\alpha}$  -  $\delta_v$  curves of RC beam-columns

(a) Bending failure



(b) Shear failure

Fig. 4 Prediction of cumulative damage of RC beam-columns

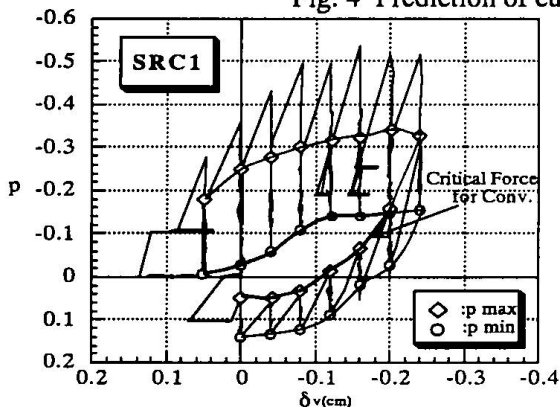
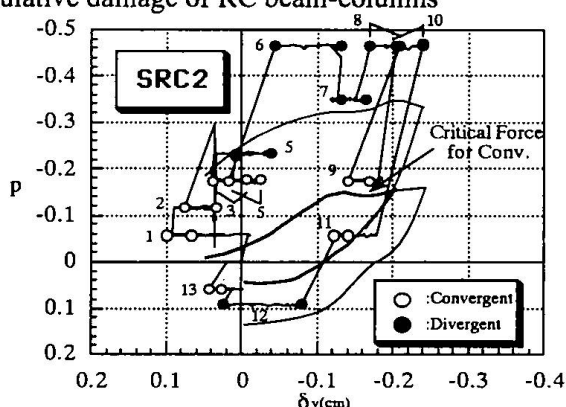
Fig. 5  $p_{\alpha}$  -  $\delta_v$  curves of SRC beam-columns

Fig. 6 Prediction of cumulative damage of SRC beam-columns

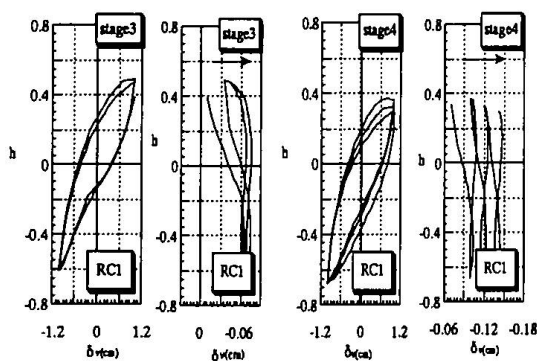
(a)  $p = -0.18$ , conv. (b)  $p = -0.26$ , div.

Fig. 7 Hysteresis loops of RC beam-columns (Bending failure type)

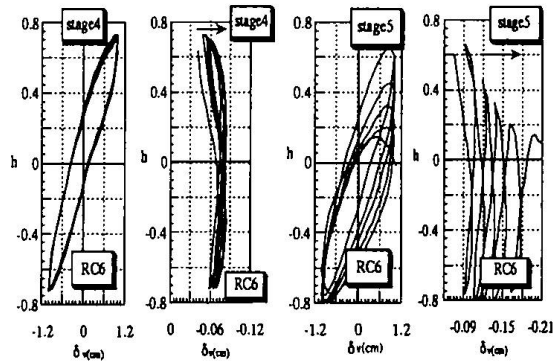
(a)  $p = -0.33$ , conv. (b)  $p = -0.41$ , div.

Fig. 8 Hysteresis loops of RC beam-columns (Shear failure type)

$$f_1(e) = \frac{e}{1 - \left(1 + \frac{2}{e_u}\right) \cdot e + \left(\frac{e}{e_u}\right)^2} \quad \text{----- } e \geq e_u, \quad f_1(e) = -1 \quad \text{----- } e < e_u$$

$$e_p = e_a \cdot \left(1 - e^{-\frac{1}{3} \left(\frac{e_a}{e_u}\right)^{15}}\right) \quad f_2(e) = -\gamma_1 \cdot f_1(e) \quad f_3(e) = -\gamma_2 \cdot f_1(e) \quad (1)$$

where  $e_a$ =strain at a common point,  $e_p$ =plastic strain.

In this analysis, the critical axial force was obtained by using the axial displacement  $\delta_v$  in the previous calculation step in the similar way to Test 2 in the experiment. Parameters listed in Tables 1 and 2 were used in analyses. Sections of concrete and steel were divided into 6 and 14 elements, respectively. Young's modulus of concrete and steel were assumed to be 210t/cm<sup>2</sup> and 2100t/cm<sup>2</sup>, respectively. Coefficients related to degrading of the s-e relation of concrete as shown in Fig. 11(b) were chosen such that  $\gamma_1=-0.7$ ,  $\gamma_2=-0.5$  for RC beam-column,  $\gamma_1=-0.4$ ,  $\gamma_2=-0.2$  for SRC beam-column. Smaller coefficients of SRC beam-column were given in view of poor casting. The amplitude of displacement  $\delta_{ha}$  was taken equal to 10mm. Eq. (2) is derived for the analytical model as shown in Fig. 10(c). The curvature at the base of beam-column can be given by Eq. (2) with the use of the displacement at the top of the beam-column  $\delta_h$ . The bending moment and the horizontal force of a beam-column were also computed from the curvature  $\Phi$ .

$$\frac{\Phi}{\Phi_y} = \frac{\delta_h}{\delta_{hy}} \quad (2)$$

where  $\Phi_y$  and  $\delta_{hy}$  are  $\Phi$  and  $\delta_h$  at the yield point, respectively.

Critical axial force  $p_{cr}$ -axial displacement  $\delta_v$  relations of RC and SRC specimens derived by analyses are shown in Fig. 11 in cases of Models A and B together with those by tests.  $p_{cr}$ - $\delta_v$  relations obtained by analyses mostly agree with test results.

#### 4. Conclusions

- 1) Cumulative damage of SRC and RC beam-columns subjected to repeated horizontal loading can be predicted by critical axial force-axial displacement relation experimentally and analytically.
- 2) Critical axial force-axial displacement relation forms hysteresis. Limit point of the curve and the slope of the descending curve represents the resisting capacity of the beam-column for cumulative damage.
- 3) The critical axial force-axial displacement relation is useful for the limitation of axial force of SRC and RC beam-columns in order to keep the aseismic safety.

#### References

- Architectural Institute of Japan (1987). AIJ Standards for Structural Calculation of Steel Reinforced Concrete Structures.
- Uchida, Y. (1996). Estimation of cumulative damage of beam-columns and frames subjected to repeated loading, Proceedings of 11WCEE, CD-ROM.

#### Acknowledgment

The authors wish to express sincere gratitude to the former students, Mr. M. Usuyama for their help in the experimental work. This research was funded by a grant-in-aid of education ministry, Japan.